Journal of Computational and Applied Mathematics 33 (1990) 1–27
North-Holland

Matrix-dependent prolongations and restrictions in a blackbox multigrid solver

P.M. DE ZEEUW
Department of Numerical Mathematics, Centre for Mathematics and Computer Science, P.O. Box 4079, 1009 AB Amsterdam, Netherlands

Received 22 June 1989
Revised 5 April 1990

Abstract: Multigrid methods are studied for the solution of linear systems resulting from the 9-point discretization of a general linear second-order elliptic partial differential equation in two dimensions. The rate of convergence of standard multigrid methods often deteriorates when the coefficients in the differential equation are discontinuous, or when dominating first-order terms are present. These difficulties may be overcome by choosing the prolongation and restriction operators in a special way. A novel way to do this is proposed. As a result, a blackbox solver (written in standard FORTRAN 77) has been developed.

Numerical experiments for several hard test problems are described and comparison is made with other algorithms: the standard MG method and a method introduced by Kettler. A significant improvement of robustness and efficiency is found.

Keywords: Convection-diffusion equation, diffusion equation, discontinuous coefficients, elliptic PDEs, Galerkin approximation, ILLU relaxation, matrix-dependent prolongation, multigrid method, sparse linear systems.

1. Introduction

Consider the partial differential equation

$$Lu \equiv -\nabla \cdot (D(x)\ \nabla u(x)) + b(x) \cdot \nabla u(x) + c(x)u(x) = f(x) \tag{1.1}$$

on a bounded domain $\Omega \subset \mathbb{R}^2$ with suitable boundary conditions. $D(x)$ is a positive definite 2×2 matrix function and $c(x) \geqslant 0$. $D(x)$, $c(x)$ and $f(x)$ are allowed to be discontinuous across internal boundaries in Ω. As a consequence $\nabla u(x)$ is discontinuous, so that in multigrid methods the use of linear interpolation for prolongation is inaccurate and leads to deterioration of the rate of convergence. In [1,7,8] prolongations are introduced that are based on continuity of $D\nabla u$ instead of continuity of ∇u. See also [3].

Another possible cause of deterioration of multigrid rate of convergence is dominance of the convection term in (1.1); roughly speaking $h \| b \| > \| D \|$, with h the mesh-size. In that case piecewise (bi)linear prolongation and the corresponding restriction yield coarse grid Galerkin approximations of the fine grid matrix in which the codiagonals dominate the main diagonal severely, even if the fine grid matrix is an M-matrix (cf. [14]). Coarse grid upwind finite-difference approximation is not a sufficient remedy, because the order of approximation by which the coarse grid operators approximate their finer counterparts is too low (cf. [14]). The purpose of this paper is to propose a new prolongation and restriction that overcome the two difficulties just mentioned, and lead to an efficient and robust blackbox multigrid code.

Section 2 contains a brief description of the sawtooth MGCS algorithm (cf. [5,10,12]) and definitions of operators used in the sections to follow. Section 3 briefly identifies some desirable relations among prolongations, restrictions and coarse grid matrices. In Section 4 the cause of failure of bilinear prolongation is discussed. A novel prolongation is presented in Section 5. Certain properties of the fine grid matrix are shown to be inherited by its coarse grid Galerkin approximation. Section 6 briefly describes the implementation and performance of a new blackbox multigrid solver based on the new prolongation. Numerical results for several hard problems appear in Section 7 where comparison is made with an MG method based on the classical bilinear prolongation and the method introduced by Kettler (cf. [7, §2.2]). In the last section conclusions are summarized.

2. Definitions

For the description of the multigrid method we introduce the following notation:

$l \in \mathbb{N}$	is the number of grids;
$h_l = h \in \mathbb{R}$	is the mesh size of the finest grids;
$h_k = 2h_{k+1},\ k = l-1,\ldots,1,$	is the mesh size on grid k;
$Z_k = \{(x_1, x_2) \mid x_1 = ih_k,\ x_2 = jh_k,\ (i, j) \in \mathbb{Z} \times \mathbb{Z}\};$	
$\Omega_k = \bar{\Omega} \cap Z_k,\ k = 1,\ldots,l,$	are the grids employed;
$U_k : \Omega_k \to \mathbb{R}$	is the set of grid functions on Ω_k;
$P_{k+1} : U_k \to U_{k+1}$	is a prolongation operator; (2.1)
$R_k : U_{k+1} \to U_k$	is a restriction operator;
$\alpha_k \in U_k$	is the grid function which takes the constant value α at all $x \in \Omega_k$;
$L_k : U_k \to U_k$	is a discrete approximation of L; L_l is the given discretization of L, with a 9-point stencil, on the finest grid; L_k, $k = l-1,\ldots,1$, is also a coarse grid approximation of L_{k+1}.

We assume that D, c and f are discontinuous only along parts of grid lines of the finest grid Ω_l. The fine grid problem to be solved is

$$L_l u_l = f_l. \tag{2.2}$$

A quasi Algol description of the "sawtooth MGCS cycle" (cf. [12,5,10]) (which is a MGCS cycle (cf. [2]) with a single smoothing step after the coarse grid correction) is as follows:

```
procedure SAWTOOTH MGCS CYCLE (f_l, L_l, u_l)
begin
 (1) f_{l-1} := R_{l-1}(f_l - L_l u_l)
 (2) for k from l-1 by -1 to 2
 (3) do f_{k-1} := R_{k-1} f_k
 (4) end do
 (5) SOLVE (f_1, L_1, u_1)
 (6) for k from 2 by 1 to l-1
 (7) do u_k := P_k u_{k-1}                                   (2.3)
 (8)     SMOOTH (f_k, L_k, u_k)
 (9) end do
(10) u_l := u_l + P_l u_{l-1}
(11) SMOOTH (f_l, L_l, u_l)
end procedure
```

In the present paper the Incomplete Line LU decomposition relaxation (ILLU) is used for SMOOTH($\cdot$). This relaxation appears to be very robust (cf. [7]); a description can be found in [5,10]. Finally we give some additional notations that will be used throughout the paper.

The grid Ω_k is split in four disjunct subgrids in the following way (a four-colour division):

$$\begin{aligned}
&\Omega_{k,(0,0)} \equiv \Omega_{k-1},\\
&\Omega_{k,(1,0)} \equiv \{(x_1 + h_k,\ x_2) \in \Omega_k \mid (x_1,\ x_2) \in \Omega_{k,(0,0)}\},\\
&\Omega_{k,(0,1)} \equiv \{(x_1,\ x_2 + h_k) \in \Omega_k \mid (x_1,\ x_2) \in \Omega_{k,(0,0)}\},\\
&\Omega_{k,(1,1)} \equiv \{(x_1 + h_k,\ x_2 + h_k) \in \Omega_k \mid (x_1,\ x_2) \in \Omega_{k,(0,0)}\}.
\end{aligned} \tag{2.4}$$

Furthermore, we need the following operators: $I_k : U_k \to U_k$, the identity operator on grid k, $I_k^{mn} : U_k \to U_k$ ($m, n = 0, 1$), a colour selection operator defined by

$$(I_k^{mn} u_k)(x_1,\ x_2) = \begin{cases} u_k(x_1,\ x_2) & \text{if } (x_1,\ x_2) \in \Omega_{k,(m,n)},\\ 0 & \text{if } (x_1,\ x_2) \notin \Omega_{k,(m,n)}. \end{cases}$$

3. Relations among prolongations, restrictions and coarse grid approximations

In (2.3) we still have to select operators P_k, R_{k-1} and L_{k-1} ($k = 2, \ldots, l$). First of all, we choose

$$R_{k-1} = P_k^{\mathrm{T}} \tag{3.1a}$$

and

$$L_{k-1} = R_{k-1} L_k P_k, \quad k = 2, \ldots, l. \tag{3.1b}$$

Equation (3.1b) is called coarse grid Galerkin approximation because

$$(L_{k-1} u_{k-1},\ v_{k-1})_{k-1} = (L_k P_k u_{k-1},\ P_k v_{k-1})_k \quad \forall u_{k-1},\ v_{k-1} \in U_{k-1}, \tag{3.2}$$

with $(\cdot,\ \cdot)_k$ the usual inner product on U_k.

Useful consequences of (3.1) are:

(i) L_k is symmetric $\Rightarrow L_{k-1}$ is symmetric.

(ii) In (2.3), if $L_{k-1} u_{k-1} = f_{k-1}$ holds just before stage (7) (if $k < l$) or (10) (if $k = l$), then $R_{k-1}(f_k - L_k u_k) = 0_{k-1}$ holds just after stage (7) (stage (10)). So, if R_{k-1} has only nonnegative entries, then after the coarse grid correction the residual of u_k consists mainly of short wavelength components, and can be reduced efficiently by the subsequent smoothing step.

(iii) Once P_k has been chosen, R_{k-1} and L_{k-1} follow automatically.

4. Bilinear prolongation

The restriction R_{k-1} and coarse grid operator L_{k-1} being defined by (3.1), we still have to choose P_k. As a start we consider bilinear interpolation defined by

$$(P_k u_{k-1})(x)$$

$$= \begin{cases} u_{k-1}(x) & \text{if } x \in \Omega_{k,(0,0)}, \\ \frac{1}{2}u_{k-1}(x+h_k(-1,0)) + \frac{1}{2}u_{k-1}(x+h_k(1,0)) & \text{if } x \in \Omega_{k,(1,0)}, \\ \frac{1}{2}u_{k-1}(x+h_k(1,0)) + \frac{1}{2}u_{k-1}(x+h_k(0,-1)) & \text{if } x \in \Omega_{k,(0,1)}, \\ \frac{1}{4}u_{k-1}(x+h_k(-1,1)) + \frac{1}{4}u_{k-1}(x+h_k(1,1)) & \\ \quad + \frac{1}{4}u_{k-1}(x+h_k(-1,-1)) + \frac{1}{4}u_{k-1}(x+h_k(1,-1)) & \text{if } x \in \Omega_{k,(1,1)}. \end{cases} \tag{4.1}$$

This prolongation can conveniently be represented by the following stencil (cf. [4, §3.4.2]):

$$\begin{bmatrix} \frac{1}{4} & \frac{1}{2} & \frac{1}{4} \\ \frac{1}{2} & 1 & \frac{1}{2} \\ \frac{1}{4} & \frac{1}{2} & \frac{1}{4} \end{bmatrix}. \tag{4.2}$$

This stencil shows the nonzero values of the fine grid function generated by prolongation of a coarse grid function which equals 1 at one point and 0 elsewhere. The prolongation (4.1) corresponds to interpolation of grid functions in U_k by a bilinear polynomial.

For a large class of problems this prolongation is quite satisfactory, but not so when the difficulties (discontinuous D or strong convection) mentioned in Section 1 occur.

4.1. Discontinuous diffusion coefficients

Consider problems with diffusion coefficients that have strong discontinuities (e.g., Problems 3–8 in Section 7). Let u_l be an approximate solution of (2.2) after a smoothing step. Consider the equation on the error

$$r_l = L_l e_l, \tag{4.3}$$

with r_l the residual of u_l and e_l the corresponding error. The effect of a smoothing step is smoothing of the residual. In case of continuous coefficients and a proper discretization (i.e., L_l is a diagonally dominant L-matrix (cf. [13]), this coincides with a smooth e_l, which can be approximated adequately by bilinear interpolation of a coarse grid function. Near a discontinuity of the diffusion coefficients a smooth r_l corresponds with an e_l with discontinuous gradient, so that e_l is not approximated well enough by bilinear interpolation of a coarse grid function. This leads to deterioration of the rate of convergence of standard multigrid methods. Therefore, alternative prolongations ([1,7,8] and the present paper) are needed.

*4.2. Dominant convection (*i.e. $\|b\|h > \|D\|$*)*

A dominant convection term, combined with a large number of grids may also lead to deterioration of rate of convergence of multigrid methods (cf. [14]). To explain why, we neglect boundary conditions (i.e., $\Omega = \mathbb{R}^2$) and consider the constant-coefficient case (i.e., L_k is a Toeplitz matrix and can be represented by one single stencil). For a stencil corresponding with

the operator Z we use the following notation:

$$Z^* = \begin{bmatrix} z_7 & z_8 & z_9 \\ z_4 & z_5 & z_6 \\ z_1 & z_2 & z_3 \end{bmatrix}. \tag{4.4}$$

This stencil can also be identified with a vector $(z_i) \in \mathbb{R}^9$.

Lemma 4.1. *Let $L_k^* \in \mathbb{R}^9$ be the stencil that represents L_k on Ω_k, and let L_{k-1} be defined by* (3.1) *and* (4.1). *Then*

(i) *a matrix $G \in \mathbb{R}^9 \times \mathbb{R}^9$ exists such that for all $L_k^* \in \mathbb{R}^9$*

$$L_{k-1}^* = GL_k^*; \tag{4.5}$$

(ii) *an eigenvalue decomposition of G exists and reads*:

$$G = VDV^{-1}, \quad G, V, D \in \mathbb{R}^9 \times \mathbb{R}^9. \tag{4.6}$$

D is a diagonal matrix representing the eigenvalues of G. The column vectors of V are the right-eigenvectors of G, the row vectors of V^{-1} are the left-eigenvectors of G.

$$V = \begin{pmatrix} -\frac{1}{6} & -\frac{1}{6} & -\frac{1}{4} & -\frac{1}{12} & -\frac{1}{12} & \frac{1}{36} & 1 & 1 & 1 \\ \frac{1}{3} & -\frac{2}{3} & 0 & 0 & -\frac{1}{3} & \frac{1}{9} & -2 & 0 & -2 \\ -\frac{1}{6} & -\frac{1}{6} & \frac{1}{4} & \frac{1}{12} & -\frac{1}{12} & \frac{1}{36} & 1 & -1 & 1 \\ -\frac{2}{3} & \frac{1}{3} & 0 & -\frac{1}{3} & 0 & \frac{1}{9} & 0 & -2 & -2 \\ \frac{4}{3} & \frac{4}{3} & 0 & 0 & 0 & \frac{4}{9} & 0 & 0 & 4 \\ -\frac{2}{3} & \frac{1}{3} & 0 & \frac{1}{3} & 0 & \frac{1}{9} & 0 & 2 & -2 \\ -\frac{1}{6} & -\frac{1}{6} & \frac{1}{4} & -\frac{1}{12} & \frac{1}{12} & \frac{1}{36} & -1 & 1 & 1 \\ \frac{1}{3} & -\frac{2}{3} & 0 & 0 & \frac{1}{3} & \frac{1}{9} & 2 & 0 & -2 \\ -\frac{1}{6} & -\frac{1}{6} & -\frac{1}{4} & \frac{1}{12} & \frac{1}{12} & \frac{1}{36} & -1 & -1 & 1 \end{pmatrix}, \tag{4.7}$$

$$V^{-1} = \begin{pmatrix} -\frac{1}{3} & \frac{1}{6} & -\frac{1}{3} & -\frac{1}{3} & \frac{1}{6} & -\frac{1}{3} & -\frac{1}{3} & \frac{1}{6} & -\frac{1}{3} \\ -\frac{1}{3} & -\frac{1}{3} & -\frac{1}{3} & \frac{1}{6} & \frac{1}{6} & \frac{1}{6} & -\frac{1}{3} & -\frac{1}{3} & -\frac{1}{3} \\ -1 & 0 & 1 & 0 & 0 & 0 & 1 & 0 & -1 \\ -1 & 0 & 1 & -1 & 0 & 1 & -1 & 0 & 1 \\ -1 & -1 & -1 & 0 & 0 & 0 & 1 & 1 & 1 \\ 1 & 1 & 1 & 1 & 1 & 1 & 1 & 1 & 1 \\ \frac{1}{6} & -\frac{1}{12} & \frac{1}{6} & 0 & 0 & 0 & -\frac{1}{6} & \frac{1}{12} & -\frac{1}{6} \\ \frac{1}{6} & 0 & -\frac{1}{6} & -\frac{1}{12} & 0 & \frac{1}{12} & \frac{1}{6} & 0 & -\frac{1}{6} \\ \frac{1}{9} & -\frac{1}{18} & \frac{1}{9} & -\frac{1}{18} & \frac{1}{36} & -\frac{1}{18} & \frac{1}{9} & -\frac{1}{18} & \frac{1}{9} \end{pmatrix} \tag{4.8}$$

and

$$D = \begin{pmatrix} 1 & & & & & & & & 0 \\ & 1 & & & & & & & \\ & & 1 & & & & & & \\ & & & 2 & & & & & \\ & & & & 2 & & & & \\ & & & & & 4 & & & \\ & & & & & & \frac{1}{2} & & \\ & & & & & & & \frac{1}{2} & \\ 0 & & & & & & & & \frac{1}{4} \end{pmatrix}. \tag{4.9}$$

Proof. Part (i) follows from a tedious evaluation of (3.1) with P_k defined by (4.2) for constant coefficients. Once G has been constructed, part (ii) can easily be verified. □

Remark 4.2. The eigenvectors of G correspond to second-order finite-difference stencils. With $V_{,j}$ the jth column of V, we see

$$V_{,1}^* \sim -h^2 \frac{\partial^2}{\partial x_1^2}, \quad V_{,2}^* \sim -h^2 \frac{\partial^2}{\partial x_2^2}, \quad V_{,3}^* \sim -h^2 \frac{\partial^2}{\partial x_1 \partial x_2},$$

$$V_{,4}^* \sim h \frac{\partial}{\partial x_1}, \quad V_{,5}^* \sim h \frac{\partial}{\partial x_2}, \quad V_{,6}^* \sim \text{identity},$$

$$V_{,7}^* \sim -2h^3 \frac{\partial^3}{\partial x_2 \partial x_1^2}, \quad V_{,8}^* \sim -2h^3 \frac{\partial^3}{\partial x_1 \partial x_2^2}, \quad V_{,9}^* \sim h^4 \frac{\partial^4}{\partial x_1^2 \partial x_2^2},$$

e.g.,

$$V_{,4}^* = \begin{bmatrix} v_{74} & v_{84} & v_{94} \\ v_{44} & v_{54} & v_{64} \\ v_{14} & v_{24} & v_{34} \end{bmatrix} = \begin{bmatrix} -\frac{1}{12} & 0 & \frac{1}{12} \\ -\frac{1}{3} & 0 & \frac{1}{3} \\ -\frac{1}{12} & 0 & \frac{1}{12} \end{bmatrix} \sim h \frac{\partial}{\partial x_1}.$$

Note that $V_{,1}^*, \ldots, V_{,6}^*$ can be obtained by discretizing by means of bilinear finite elements on a regular grid with meshsize h.

By repeatedly applying (3.1) (and (4.1)) we obtain a coarse grid operator L_{k-n}, $n > 0$, for which the following holds.

Remark 4.3.

$$L_{k-n}^* = G^n L_k^* = \sum_{i=1}^{9} d_i^m \alpha_i V_{,i},$$

where d_i is the ith eigenvalue of G and $\alpha_i \equiv w_{i\cdot} L_k^*$, where $w_{i\cdot}$ denotes the ith row of V^{-1} and $\cdot$ denotes the usual inner product on $\mathbb{R}^9$.

This can easily be seen because $\{V_{,i}\}_{i=1,\ldots,9}$ is a linear independent set of vectors and L_k^* can be written as

$$L_k^* = \sum_{i=1}^{9} \alpha_i V_{,i},$$

with α_i, $i = 1,\ldots,9$, uniquely defined.

Now we consider the case of a simple convection-diffusion equation for which $\alpha_6 = 0$ and $\alpha_4 \neq 0$ or $\alpha_5 \neq 0$. Because of Remark 4.3 it is obvious that the co-diagonals increase rapidly as n increases and hence diagonal dominance is lost.

Example 4.4. Let

$$L_k^* = \begin{bmatrix} 0 & 0 & 0 \\ -1 & 1 & 0 \\ 0 & 0 & 0 \end{bmatrix};$$

then

$$L_k^* = \tfrac{1}{2}V_{,1}^* + V_{,4}^* + \tfrac{1}{12}V_{,8}^* + \tfrac{1}{12}V_{,9}^*,$$

and hence

$$L_{k-n}^* = \tfrac{1}{2}V_{,1}^* + 2^n V_{,4}^* + \left(\tfrac{1}{2}\right)^n \tfrac{1}{12}V_{,8}^* + \left(\tfrac{1}{4}\right)^n \tfrac{1}{12}V_{,9}^*,$$

so L_{k-n}^* is dominated by the term $2^n V_{,4}$ for increasing n. This means that smoothing methods loose their effectiveness. The difficulty sketched in this subsection will also be overcome by means of the prolongation operator to be proposed.

5. Matrix-dependent prolongation

5.0. Introduction

We introduce the following prolongation:

$$(P_k u_{k-1})(x) = \begin{cases} u_{k-1}(x) & \text{if } x \in \Omega_{k,(0,0)}, \\ b_k(x)u_{k-1}(x + h_k(-1, 0)) + a_k(x)u_{k-1}(x + h_k(1, 0)) & \text{if } x \in \Omega_{k,(1,0)}, \\ b_k(x)u_{k-1}(x + h_k(0, 1)) + a_k(x)u_{k-1}(x + h_k(0, -1)) & \text{if } x \in \Omega_{k,(0,1)}, \\ b_k(x)u_{k-1}(x + h_k(-1, 1)) + c_k(x)u_{k-1}(x + h_k(1, 1)) & \\ + d_k(x)u_{k-1}(x + h_k(-1, -1)) + a_k(x)u_{k-1}(x + h_k(1, -1)) & \\ & \text{if } x \in \Omega_{k,(1,1)}, \end{cases} \tag{5.1}$$

$a_k, b_k, c_k, d_k \in U_k$.

This prolongation has the stencil

$$\begin{bmatrix} a_k(x+h_k(-1,1)) & a_k(x+h_k(0,1)) & d_k(x+h_k(1,1)) \\ a_k(x+h_k(-1,0)) & 1 & b_k(x+h_k(1,0)) \\ c_k(x+h_k(-1,-1)) & b_k(x+h_k(0,-1)) & b_k(x+h_k(1,-1)) \end{bmatrix}, \quad x \in \Omega_{k-1}. \tag{5.2}$$

Because of (3.1a) the stencil (5.2) also gives the weights of the restriction R_{k-1} at $x \in \Omega_{k-1}$. The original matrix L_l is assumed to correspond to a 9-point discretization. Because of (5.2) and (3.1a) all L_k, $k < l$, are 9-point discretizations as well. To complete the description of P_k in (5.1), (5.2) we have to determine the weights a_k, b_k, c_k, d_k. This will be postponed until Section 5.3. Beforehand, we show in Section 5.1 that a conservative discretization on grid Ω_k results in a conservative discretization on grid Ω_{k-1}, provided that grid function 1_{k-1} is prolongated into 1_k by P_k.

In Section 5.2 a particular prolongation of type (5.2) is introduced for the case of L having constant coefficients. The stencil of this prolongation depends on two parameters: $\lambda \in \mathbb{R}$ which makes the prolongation asymmetric in the x_1-direction and $\mu \in \mathbb{R}$ which makes it asymmetric in the x_2-direction (the case $\lambda = \mu = 0$ is the conventional bilinear prolongation). If convection is dominant, the difficulty of lack of diagonal dominance of the coarse grid matrix is met by choosing $\lambda \neq 0$, $\mu \neq 0$ by which automatically diffusion is added to the matrix at its evaluation (3.1b) (this is proven by Lemma 5.4). Finally, in Section 5.3 the prolongation is presented which has been implemented into the new blackbox solver. It is destined primarily for the case of discontinuous diffusion coefficients. Firstly, the prolongation at the subset $\Omega_{k,(1,1)}$ is defined by the discrete homogeneous equation, this is done in Section 5.3.1. Secondly, the prolongation at $\Omega_{k,(1,0)}$ and $\Omega_{k,(0,1)}$ is defined in Section 5.3.2. The weights of the prolongation at these points are derived as follows:

(i) decompose the matrix into its diffusive and its convective parts;

(ii) let $\xi \in \Omega_{k,(1,0)}$ (or $\Omega_{k,(0,1)}$) be a point where a coarse grid correction has to be interpolated, then derive the different diffusion coefficients in the neighbourhood of ξ;

(iii) based on the local character of the reconstructed differential equation, use some heuristic arguments to find appropriate prolongation weights at ξ.

In Section 5.3.3 the connection is shown between the prolongation for constant coefficients defined in Section 5.2 and the one defined for variable coefficients in Section 5.3. Here, by Lemma 5.15 it becomes clear that the prolongation in Section 5.3 is applicable also for constant coefficients and dominant convection.

5.1. Conservation of properties of the fine grid discretization on the coarse grids

In this subsection it is shown that some important properties of L_l may be inherited by L_k, $k < l$, if a condition on a_k, b_k, c_k, d_k is satisfied. For that purpose some lemmas are formulated.

Lemma 5.1. *With P_k defined by* (5.1), *it satisfies*

$$P_k 1_{k-1} = 1_k$$
$$\Leftrightarrow \begin{cases} a_k(x) + b_k(x) = 1 & \text{if } x \in \Omega_{k,(1,0)} \text{ or } x \in \Omega_{k,(0,1)}, \\ a_k(x) + b_k(x) + c_k(x) + d_k(x) = 1 & \text{if } x \in \Omega_{k,(1,1)}. \end{cases}$$

Proof. Follows by straightforward computation. □

Lemma 5.2. *Assume* $P_k 1_{k-1} = 1_k$. *Let* $f_{k-1} \equiv R_{k-1} f_k$. *Then* f_{k-1} *and* L_{k-1} *have the following properties*:

(i) *the sum of elements of* f_{k-1} *is equal to the sum of elements of* f_k;
(ii) *the sum of all entries of matrix* L_{k-1} *is equal to the sum of all entries of* L_k;
(iii) *if every row sum of matrix* L_k *equals zero, then every row sum of* L_{k-1} *equals zero*;
(iv) *if every column sum of matrix* L_k *equals zero, then every column sum of* L_{k-1} *equals zero.*

Proof.

(i) $1_{k-1}^T f_{k-1} = 1_{k-1}^T R_{k-1} f_k = (P_k 1_{k-1})^T f_k = 1_k^T f_k$.
(ii) $1_{k-1}^T L_{k-1} 1_{k-1} = 1_{k-1}^T R_{k-1} L_k P_k 1_{k-1} = (P_k 1_{k-1})^T L_k 1_k = 1_k^T L_k 1_k$.
(iii) $L_{k-1} 1_{k-1} = R_{k-1} L_k P_k 1_{k-1} = R_{k-1}(L_k 1_k) = R_{k-1} 0_k = 0_{k-1}$.
(iv) $L_{k-1}^T 1_{k-1} = (R_{k-1} L_k P_k)^T 1_{k-1} = R_{k-1} L_k^T P_k 1_{k-1} = R_{k-1}(L_k^T 1_k) = R_{k-1} 0_k = 0_{k-1}$. □

Part (iii) and (iv) can easily be generalized to the following lemma.

Lemma 5.3. *Let*

$$L_k^* \equiv \begin{bmatrix} L_k(x)(-1,1) & L_k(x)(0,1) & L_k(x)(1,1) \\ L_k(x)(-1,0) & L_k(x)(0,0) & L_k(x)(1,0) \\ L_k(x)(-1,-1) & L_k(x)(0,-1) & L_k(x)(1,-1) \end{bmatrix} \tag{5.3}$$

be the stencil of L_k *at* $x \in \Omega_k$. *Let* $\Sigma_k(x) = \sum_{j=-1}^{1} \sum_{i=-1}^{1} L_k(x)(i, j)$ (i.e., *the row sum*) *and let* $\Sigma_k'(x) = \sum_{j=-1}^{1} \sum_{i=-1}^{1} L_k^T(x)(i, j)$ (i.e., *the column sum*). *Let* $x_0 \in \Omega_{k-1}$ *and* $S(x_0) = \{x_0 + h_k(i, j) \mid |i| \leqslant 1, |j| \leqslant 1\}$. *If* $(P_k 1_{k-1})(x) = 1$ *for all* $x \in S(x_0)$, *then the following holds*:

(i) $\Sigma_k(x) = 0$ *for all* $x \in S(x_0) \Rightarrow \Sigma_{k-1}(x_0) = 0$;
(ii) $\Sigma_k'(x) = 0$ *for all* $x \in S(x_0) \Rightarrow \Sigma_{k-1}'(x_0) = 0$.

Proof. Similar to Lemma 5.2(iii), (iv). □

The properties (i), (iii), (iv) mentioned in Lemma 5.2 make sense e.g. for Problems 1, 4, 6 in Section 7, which are pure diffusion problems with homogeneous Neumann boundary conditions only. By a conservative discretization, the linear systems $L_l u_l = f_l$ that arise have the properties:
- L_l is symmetric,
- the sum of elements of f_l vanishes,
- every row sum of L_l equals zero,
- every column sum of L_l equals zero.

For all $k \leqslant l$, let P_k be such that $P_k 1_{k-1} = 1_k$. Because of consequence (i) in Section 3 and Lemma 5.2 it is clear that the properties of L_l and f_l mentioned above are inherited by L_k and f_k for all $k < l$. (For problems with Dirichlet boundary conditions, Lemma 5.3 can be applied.) Of course, all L_k, $k \leqslant l$, are singular. However, all systems $L_k u_k = f_k$ are solvable because for each k, f_k is within the range of L_k, i.e., the sum of its elements equals zero. The solution is unique up to a constant.

We conclude that for systems of the above-mentioned type it is favorable to use prolongations which satisfy $P_k 1_{k-1} = 1_k$.

5.2. Matrix-dependent prolongation for the constant-coefficient case

Assume that L has constant coefficients; then the prolongation

$$P_k(\lambda,\mu)\equiv\begin{bmatrix}\frac14&\frac12&\frac14\\ \frac12&1&\frac12\\ \frac14&\frac12&\frac14\end{bmatrix}+\lambda\begin{bmatrix}-\frac12&0&\frac12\\ -1&0&1\\ -\frac12&0&\frac12\end{bmatrix}+\mu\begin{bmatrix}\frac12&1&\frac12\\ 0&0&0\\ -\frac12&-1&-\frac12\end{bmatrix}, \tag{5.4}$$

with $\lambda,\mu\in[-\frac12,+\frac12]$ is considered for grid functions on $\Omega_k-\partial\Omega$. Both λ and μ remain to be chosen.

Let $(l_i)\equiv L_k^*$ denote the stencil of L_k. Possible choices for λ and μ are:

(i) $\lambda\equiv\dfrac{l_4-l_6}{2(l_4+l_6)}$, $\quad\mu\equiv\dfrac{l_2-l_8}{2(l_2+l_8)}$

(this coincides with the prolongation used in [7] except for $\Omega_{k,(1,1)}$ points);

(ii) $\lambda\equiv\dfrac{(l_1+l_4+l_7)-(l_3+l_6+l_9)}{2((l_1+l_4+l_7)+(l_3+l_6+l_9))}$, $\quad\mu$ analogously

(this coincides with the prolongation used in [3] except for the $\Omega_{k,(1,1)}$ points);

(iii) $\lambda\equiv\dfrac{w_4\cdot L_k^*}{4w_1\cdot L_k^*}$, $\quad\mu\equiv\dfrac{w_5\cdot L_k^*}{4w_2\cdot L_k^*}$

with w_i and $\cdot$ as in Remark 4.3. Here the asymmetry in the prolongation is proportional to the ratio of convection and diffusion in the x_1- and x_2-direction, respectively.

Clearly, P_k satisfies the condition that $P_k 1_{k-1}=1_k$. For (5.4) the following lemma holds.

Lemma 5.4. (i) *A matrix* $G(\lambda,\mu)\in\mathbb{R}^9\times\mathbb{R}^9$ *exists such that*

$$L_{k-1}^*=G(\lambda,\mu)L_k^*$$

for all $L_k^*\in\mathbb{R}^9$.

(ii) *With* V *defined by* (4.7), $\tilde D\equiv V^{-1}G(\lambda,\mu)V$ *is given by*

$$\tilde D=\begin{pmatrix}1+4\lambda^2&0&0&0&0&\frac43\lambda^2&0&0&0\\ 0&1+4\mu^2&0&0&0&\frac43\mu^2&0&0&0\\ 0&0&1&0&0&2\lambda\mu&0&0&0\\ 0&0&0&2&0&0&0&0&0\\ 0&0&0&0&2&0&0&0&0\\ 0&0&0&0&0&4&0&0&0\\ 0&0&0&\frac12\lambda\mu&\frac13\lambda^2&0&\frac12+2\lambda^2&0&0\\ 0&0&0&\frac13\mu^2&\frac12\lambda\mu&0&0&\frac12+2\mu^2&0\\ \frac13\mu^2&\frac13\lambda^2&\frac12\lambda\mu&0&0&0&0&0&\frac14+\lambda^2+\mu^2\end{pmatrix}. \tag{5.5}$$

Proof. Part (i) follows from a straightforward but tedious evaluation of (3.1). Once $G(\lambda,\mu)$ has been constructed, part (ii) can easily be verified. □

This $\tilde{D}(\lambda, \mu)$ is a generalization of D in (4.9) for the case $(\lambda, \mu) \neq (0, 0)$. The columns of $\tilde{D}$ describe how a stencil corresponding to vector $v_{,i}$, $i = 1, \ldots, 9$, is transformed, e.g.,

$$G(\lambda, \mu)v_{,1} = (1 + 4\lambda^2)v_{,1} + \tfrac{1}{3}\mu^2 v_{,9},$$

$$G(\lambda, \mu)v_{,4} = 2v_{,4} + \tfrac{1}{2}\lambda\mu v_{,7} + \tfrac{1}{3}\mu^2 v_{,8}, \quad \text{etc.}$$

Example 5.5 (Cf. Example 4.4). Let

$$L_k^* = \begin{bmatrix} 0 & 0 & 0 \\ -1 & 1 & 0 \\ 0 & 0 & 0 \end{bmatrix};$$

then

$$L_k^* = \tfrac{1}{2}v_{,1}^* + v_{,4}^* + \tfrac{1}{12}v_{,8}^* + \tfrac{1}{12}v_{,9}^*,$$

and, if $L_{k-n}^* = G^n(\lambda, 0)L_k^*$, then

$$L_{k-n}^* = (1 + 4\lambda^2)^n \tfrac{1}{2}v_{,1}^* + 2^n v_{,4}^* + \left(\tfrac{1}{2}\right)^n \tfrac{1}{12}v_{,8}^* + \left(\tfrac{1}{4} + \lambda^2\right)^n \tfrac{1}{12}v_{,9}^*.$$

Apparently, by $\lambda \neq 0$ extra diffusion is added to the coarse grid approximation of the stencil.

5.3. Matrix-dependent prolongation in the case of discontinuous coefficients

In this subsection the prolongation is presented which has been implemented into the new blackbox solver. In order to complete the description of P_k in (5.1), (5.2) we specify the weights a_k, b_k, c_k, d_k. This is done in two steps: (i) the construction of a_k, b_k, c_k, d_k at $\Omega_{k,(1,1)}$; (ii) the construction of a_k and b_k at $\Omega_{k,(1,0)}$ and $\Omega_{k,(0,1)}$.

5.3.1. The weights at $\Omega_{k,(1,1)}$

Assume that a_k and b_k at $\Omega_{k,(1,0)}$ and $\Omega_{k,(0,1)}$ have already been chosen. Let r_k be the residual before and $\tilde{r}_k$ be the residual of u_k after adding the coarse grid correction $P_k u_{k-1}$ (see Section 2); then the equality

$$\tilde{r}_k = r_k - L_k P_k u_{k-1} \tag{5.6}$$

holds. In order to prevent huge jumps in the l_2-norm of the residual after interpolation (cf. [1, p.437]), we require

$$I_k^{11}(L_k P_k u_{k-1}) = 0_k \quad \forall u_{k-1} \in U_{k-1}. \tag{5.7}$$

Hence

$$\sum_{j=-1}^{1} \sum_{i=-1}^{1} L_k(x)(i, j)(P_k u_{k-1})(x + h_k(i, j)) = 0, \quad x \in \Omega_{k,(1,1)}, \tag{5.8}$$

(where $L_k(x)(i, j)$ as in (5.3)).

Substituting the weights a_k and b_k at $\Omega_{k,(1,0)}$ and $\Omega_{k,(0,1)}$ as given in (5.1) we obtain

$$\begin{aligned}
a_k(x) &= -\{L_k(x)(1,-1) + L_k(x)(0,-1)a_k(x+h_k(0,-1)) \\
&\quad + L_k(x)(1,0)a_k(x+h_k(1,0))\}[L_k(x)(0,0)]^{-1}, \\
b_k(x) &= -\{L_k(x)(-1,1) + L_k(x)(-1,0)b_k(x+h_k(-1,0)) \\
&\quad + L_k(x)(0,1)b_k(x+h_k(0,1))\}[L_k(x)(0,0)]^{-1}, \\
c_k(x) &= -\{L_k(x)(1,1) + L_k(x)(1,0)b_k(x+h_k(1,0)) \\
&\quad + L_k(x)(0,1)a_k(x+h_k(0,1))\}[L_k(x)(0,0)]^{-1}, \\
d_k(x) &= -\{L_k(x)(-1,-1) + L_k(x)(0,-1)b_k(x+h_k(0,-1)) \\
&\quad + L_k(x)(-1,0)a_k(x+h_k(-1,0))\}[L_k(x)(0,0)]^{-1},
\end{aligned} \tag{5.9}$$

for $x \in \Omega_{k,(1,1)}$. (It is assumed that $L_k(x)(0,0) \neq 0$.) These weights are in effect computed in the blackbox solver.

Lemma 5.6. *Let* $x \in \Omega_{k,(1,1)}$, $k \leqslant l$. *If* $b_k(x + h_k z) + a_k(x + h_k z) = 1$ *for* $z \in \{(-1,0),(1,0),(0,-1),(0,1)\}$ *and* $L_k(x)(0,0) \neq 0$ *we find*

$$a_k(x) + b_k(x) + c_k(x) + d_k(x) = 1 - \frac{\Sigma_k(x)}{L_k(x)(0,0)},$$

where $\Sigma_k(x)$ *again denotes the row sum* (cf. *Lemma* 5.3). *In addition, if* $L_k(x)(i,j) \leqslant 0$ *for* $(i,j) \neq (0,0)$ *and* $L_k(x)(0,0) > 0$ *and both* $b_k(x + h_k z)$, $a_k(x + h_k z) \geqslant 0$, *then* $a_k(x)$, $b_k(x)$, $c_k(x)$, $d_k(x) \geqslant 0$.

Proof. The lemma follows immediately from (5.9). □

This lemma combined with Lemma 5.1 indicates that if (i) the weights of the prolongation on the horizontal (vertical) coarse grid lines are defined such that on those lines 1_{k-1} is prolongated into 1_k, (ii) the row sums of matrix L_k equal zero, then P_k is such that $P_k 1_{k-1} = 1_k$, which generates nice properties for the coarse grid systems as explained in Section 5.1.

5.3.2. The weights at $\Omega_{k,(1,0)}$ and $\Omega_{k,(0,1)}$

These weights are found by an approximate reconstruction of the continuous equation at the grid points, using the information which is available from L_k. We proceed as follows. Let

$$\begin{aligned}
S_k &\equiv \tfrac{1}{2}(L_k + L_k^{\mathrm{T}}), \\
A_k &\equiv \tfrac{1}{2}(L_k - L_k^{\mathrm{T}}).
\end{aligned} \tag{5.10}$$

This corresponds to splitting the stencil of L_k at $x \in \Omega_k$ as follows:

$$\begin{aligned}
L_k(x)(i,j) &= S_k(x)(i,j) + A_k(x)(i,j), \\
S_k(x)(i,j) &= \tfrac{1}{2}(L_k(x)(i,j) + L_k(x+h_k(i,j))(-i,-j)), \\
A_k(x)(i,j) &= \tfrac{1}{2}(L_k(x)(i,j) - L_k(x+h_k(i,j))(-i,-j)),
\end{aligned} \tag{5.11}$$

$|i| \leqslant 1$, $|j| \leqslant 1$. It is natural to assume that S_k originates from the diffusion and zeroth order terms of (1.1), while A_k originates from the convection terms. Equation (5.11) is rewritten as:

$$\begin{bmatrix} l_7 & l_8 & l_9 \\ l_4 & l_5 & l_6 \\ l_1 & l_2 & l_3 \end{bmatrix} = \begin{bmatrix} s_7 & s_8 & s_9 \\ s_4 & s_5 & s_6 \\ s_1 & s_2 & s_3 \end{bmatrix} + \begin{bmatrix} a_7 & a_8 & a_9 \\ a_4 & a_5 & a_6 \\ a_1 & a_2 & a_3 \end{bmatrix}. \tag{5.12}$$

Of course, $s_5 = l_5$ and $a_5 = 0$. The symmetric part is decomposed by

$$\begin{aligned} \begin{bmatrix} s_7 & s_8 & s_9 \\ s_4 & s_5 & s_6 \\ s_1 & s_2 & s_3 \end{bmatrix} = & -s_{147}\begin{bmatrix} 0 & 0 & 0 \\ -1 & 1 & 0 \\ 0 & 0 & 0 \end{bmatrix} - s_{369}\begin{bmatrix} 0 & 0 & 0 \\ 0 & 1 & -1 \\ 0 & 0 & 0 \end{bmatrix} - s_{123}\begin{bmatrix} 0 & 0 & 0 \\ 0 & 1 & 0 \\ 0 & -1 & 0 \end{bmatrix} \\ & - s_{789}\begin{bmatrix} 0 & -1 & 0 \\ 0 & 1 & 0 \\ 0 & 0 & 0 \end{bmatrix} - s_1\begin{bmatrix} 0 & 0 & 0 \\ 1 & -1 & 0 \\ -1 & 1 & 0 \end{bmatrix} + s_7\begin{bmatrix} 1 & -1 & 0 \\ -1 & 1 & 0 \\ 0 & 0 & 0 \end{bmatrix} \\ & + s_3\begin{bmatrix} 0 & 0 & 0 \\ 0 & 1 & -1 \\ 0 & -1 & 1 \end{bmatrix} - s_9\begin{bmatrix} 0 & 1 & -1 \\ 0 & -1 & 1 \\ 0 & 0 & 0 \end{bmatrix} + \Sigma\begin{bmatrix} 0 & 0 & 0 \\ 0 & 1 & 0 \\ 0 & 0 & 0 \end{bmatrix}, \end{aligned} \tag{5.13}$$

where $s_{pqr} \equiv s_p + s_q + s_r$ and $\Sigma \equiv \sum_{i=1}^{9} s_i$.

We can identify the elementary stencils in the right-hand side of (5.13) as contributions from a symmetric differential operator. Thus, schematically, the diffusion coefficients of (1.1) in the different regions near x are found to be as in Fig. 5.1.

The coefficient Σ accounts for the zero-order term. Note that the set of stencils at the right-hand side of (5.13) forms a basis of $\mathbb{R}^9$, hence the coefficients s_{147} etc. are uniquely determined. Similarly, the coefficients of $h(\partial/\partial x_1)$ and $h(\partial/\partial x_2)$ are approximated by

$$c_1 \equiv (a_3 + a_6 + a_9) - (a_1 + a_4 + a_7) \quad \text{(averaging out the } x_2\text{-dependence)}, \tag{5.15}$$

$$c_2 \equiv (a_7 + a_8 + a_9) - (a_1 + a_2 + a_3) \quad \text{(averaging out the } x_1\text{-dependence)}. \tag{5.16}$$

As far as possible we try to incorporate the information, gathered in (5.11)–(5.16), into a proper definition of the weights a_k and b_k at $\Omega_{k,(1,0)}$ and $\Omega_{k,(0,1)}$. The same procedure is followed in the

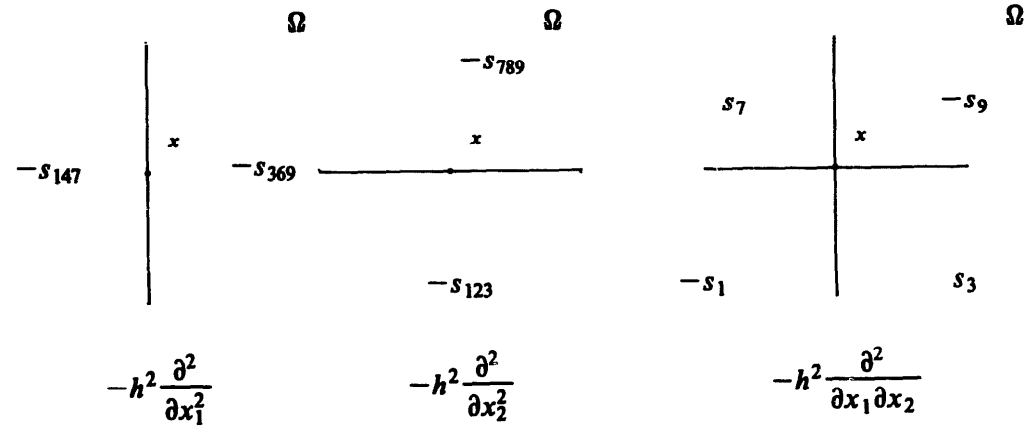

(5.14)

Fig. 5.1.

horizontal and the vertical direction, therefore we restrict the description to the weights at $\Omega_{k,(1,0)}$. We simplify the notation and write for some $x \in \Omega_{k,(1,0)}$:

$$(P_k u_{k-1})(x) = w_W u_W + w_E u_E, \tag{5.17}$$

with $u_W \equiv u_{k-1}(x + h_k(1, 0))$, $u_E = u_{k-1}(x + h_k(-1, 0))$. By (5.17), $u_k(x)$ is to be computed from u_W and u_E. To determine the weights w_W and w_E we first formulate some guidelines for their construction:

$$\text{(i)} \qquad w_W + w_E = 1 - \frac{\Sigma_k(x)}{L_k(x)(0,0)} \quad \text{and} \quad w_W, w_E \geq 0. \tag{5.18}$$

In Sections 5.1 and 5.3.1 we have seen that for any problem with $\Sigma_k(x) = 0$ we should satisfy $w_W + w_E = 1$ and $w_W, w_E \geq 0$. Another case of interest is

$$L_k(x)(i, j)\begin{cases} = 0 & \text{if}(i, j) \neq (0, 0), \\ \neq 0 & \text{if}(i, j) = (0, 0), \end{cases}$$

in which case we should have $w_W = w_E = 0$. This is an optimal choice because a (local) relaxation solves the equation at x at once and any nonzero coarse grid correction would be harmful.

(ii) In the one-dimensional case the prolongation should reduce to interpolation by means of the difference operator. This is achieved as follows. Let

$$\begin{aligned} &s_4 = -d_W, && a_4 = -\tfrac{1}{2}c_1, \\ &s_5 = d_W + d_E + \Sigma, \\ &s_6 = -d_E, && a_6 = +\tfrac{1}{2}c_1, \\ &s_i = a_i = 0 \quad \text{if } i < 4 \text{ or } i > 6; \end{aligned}$$

then take

$$w_W = \frac{d_W + \frac{1}{2}c_1}{d_W + d_E + \Sigma}, \qquad w_E = \frac{d_E - \frac{1}{2}c_1}{d_W + d_E + \Sigma}. \tag{5.19}$$

(Notice that if $c_1 = 0$ and $\Sigma = 0$, then these expressions reduce to the formula given by Hackbusch [4, §10.3.1]). In the one-dimensional case, (5.17) results in $I_k^{10} L_k P_k u_{k-1} = 0_k$.

With (i) and (ii) in mind, we propose the following formulas for w_W and w_E. Let

$$\begin{aligned} &d_W = \max(|s_{147}|, |s_1|, |s_7|), && d_E = \max(|s_{369}|, |s_3|, |s_9|), \\ &d_N = \max(|s_{789}|, |s_7|, |s_9|), && d_S = \max(|s_{123}|, |s_1|, |s_3|), \end{aligned} \tag{5.20a}$$

$$\sigma = \min\left(1, \left|1 - \frac{\Sigma}{I_5}\right|\right), \tag{5.20b}$$

$$w'_W = \sigma\left(\frac{1}{2} + \frac{1}{2}\frac{d_W - d_E}{d_W + d_E} + \frac{1}{2}\frac{c_1}{d_W + d_E + d_N + d_S}\right), \tag{5.20c}$$

$$w'_E = \sigma\left(\frac{1}{2} + \frac{1}{2}\frac{d_E - d_W}{d_W + d_E} - \frac{1}{2}\frac{c_1}{d_W + d_E + d_N + d_S}\right). \tag{5.20d}$$

Then we choose

$$w_W = \min(\sigma, \max(0, w'_W)), \tag{5.20e}$$

$$w_E = \min(\sigma, \max(0, w'_E)), \tag{5.20f}$$

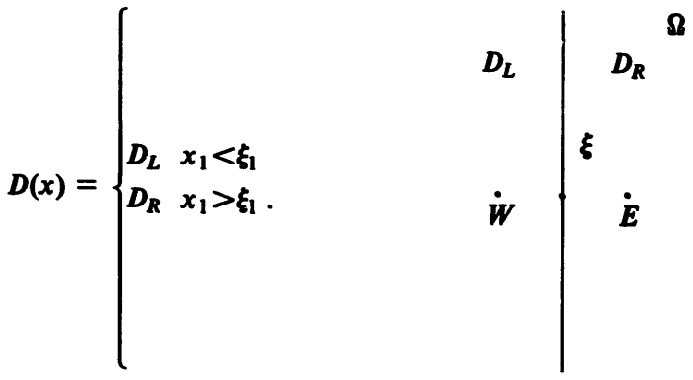

Fig. 5.2. $D(x)$ for Example 5.10.

(c_1, Σ, s_i, s_{ijk} as defined in (5.13)–(5.16)). It is easily verified that (5.20) satisfies the requirements (i) and (ii) above.

Remark 5.7. $w_W + w_E = \sigma$.

Remark 5.8. (5.20b) and (5.20e), (5.20f) have safeguards to enforce that

$$0 \leqslant w_W \leqslant \sigma \leqslant 1, \qquad 0 \leqslant w_E \leqslant \sigma \leqslant 1.$$

If L_k is a diagonally dominant L-matrix, then these safeguards are superfluous.

Remark 5.9. In (5.20a) also the coefficients of the mixed derivative are involved (see (5.14)). This is done because of the following heuristic argument. Consider d_W; if s_7 (or s_1) is not zero this implies a coupling between the values of u in the north-west (south-west) quadrant and therefore between u_W and u at ξ. Similar arguments hold for d_E, d_N, d_S. These couplings are incorporated in (5.20a). Experiments indeed showed that neglect of $|s_1|$, $|s_7|$, $|s_3|$, $|s_9|$ causes slower convergence of the multigrid algorithm.

We conclude Section 5.3 with examples of weights on horizontal gridlines resulting from the description in this section, for some special cases of interest.

Example 5.10. Let $Lu \equiv -\nabla (D \nabla u)$, see Fig. 5.2. (For the discretization of L, cf. [1].) Then

$$(P_k u_{k-1})(\xi) = w_W u_W + w_E u_E,$$

with

$$w_W = \frac{D_L}{D_L + D_R}, \qquad w_E = \frac{D_R}{D_L + D_R}.$$

Example 5.11. Let

$$Lu \equiv -\epsilon \, \Delta u + \cos \alpha \, \frac{\partial u}{\partial x} + \sin \alpha \frac{\partial u}{\partial y}, \quad \epsilon > 0.$$

Let L_l be given by the stencil

$$\begin{bmatrix} 0 & -\epsilon & 0 \\ -\cos\alpha-\epsilon & \cos\alpha+\sin\alpha+4\epsilon & -\epsilon \\ 0 & -\sin\alpha-\epsilon & 0 \end{bmatrix}, \quad 0 \leqslant \alpha \leqslant \tfrac{1}{2}\pi,$$

so that

$$S_l = \begin{bmatrix} 0 & -\frac{1}{2}\sin\alpha-\epsilon & 0 \\ -\frac{1}{2}\cos\alpha-\epsilon & \cos\alpha+\sin\alpha+4\epsilon & -\frac{1}{2}\cos\alpha-\epsilon \\ 0 & -\frac{1}{2}\sin\alpha-\epsilon & 0 \end{bmatrix} \quad \text{and}$$

$$A_l = \begin{bmatrix} 0 & +\frac{1}{2}\sin\alpha & 0 \\ -\frac{1}{2}\cos\alpha & 0 & +\frac{1}{2}\cos\alpha \\ 0 & -\frac{1}{2}\sin\alpha & 0 \end{bmatrix}.$$

Then

$$w_W = \frac{1}{2} + \frac{1}{2}\,\frac{\cos\alpha}{\cos\alpha+\sin\alpha+4\epsilon}, \qquad w_E = \frac{1}{2} - \frac{1}{2}\,\frac{\cos\alpha}{\cos\alpha+\sin\alpha+4\epsilon}.$$

Example 5.12. Let $Lu = -\epsilon\,\Delta u + \delta u$, $\epsilon > 0$. Let L_l correspond to the stencil ($h = 1$):

$$\begin{bmatrix} -\epsilon & -\epsilon & -\epsilon \\ -\epsilon & 8\epsilon+\delta & -\epsilon \\ -\epsilon & -\epsilon & -\epsilon \end{bmatrix}.$$

Then

$$w_W = w_E = \tfrac{1}{2} \quad \text{if } \delta \leqslant 0, \qquad w_W = w_E = \frac{4\epsilon}{8\epsilon+\delta} \quad \text{if } \delta > 0.$$

Example 5.13. Let

$$Lu \equiv -\Delta u + \alpha \frac{\partial^2}{\partial x_1\,\partial x_2} u$$

and let L_l correspond to

$$\begin{bmatrix} -\alpha & -1+\alpha & 0 \\ -1+\alpha & 4-\alpha & -1 \\ 0 & -1 & 0 \end{bmatrix}, \quad 0 < \alpha < 1 \text{ (cf. [4, p.217])}.$$

Then $w_W = w_E = \frac{1}{2}$.

Example 5.14. Consider the stencil

$$L_k(\xi) = \begin{bmatrix} \delta_7-\beta & \delta_8+\beta & \delta_9 \\ \delta_4+\beta & \delta_5-\beta & \delta_6 \\ \delta_1 & \delta_2 & \delta_3 \end{bmatrix}, \qquad \begin{matrix} \delta_i > 0, & i = 5, \\ \delta_i \leqslant 0, & i \neq 5, \end{matrix}$$

with $\Sigma_{i=1}^{9}\,\delta_i = 0$, for $\xi \in \Omega_{k,(1,0)}$ and with $L_k = S_k$. This situation occurs on coarser grids ($k < l$) in the following situation:

$$L \equiv -\nabla\,(D\nabla),$$

with

$$D(x) = \begin{cases} D_1, & x_1 < \xi_1 \text{ and } x_2 > \xi_2, \\ D_2, & \text{elsewhere}, \end{cases}$$

$$D_1 > D_2,$$

then

$$w_W = \frac{-\delta_1 - \delta_4 - \delta_7}{-\delta_1 - \delta_4 - \delta_7 - \delta_3 - \delta_6 - \delta_9}, \qquad w_E = 1 - w_W \quad \text{if } |\delta_7 - \beta| \leqslant -\delta_1 - \delta_4 - \delta_7,$$

$$w_E = \frac{|\delta_7 - \beta|}{|\delta_7 - \beta| - \delta_3 - \delta_6 - \delta_9}, \qquad w_E = 1 - w_W \quad \text{if } |\delta_7 - \beta| > -\delta_1 - \delta_4 - \delta_7.$$

5.3.3. The constant-coefficient case revisited

Assume that L has constant coefficients with dominant convection. We pose the question how the prolongation as described in Section 5.3.2 behaves for this case. To answer this question it is shown that there is a link with prolongation (5.4) which could be analyzed well with respect to the procreation of coarse grid matrices. Let L_k be defined by the stencil

$$L_k^* \equiv \begin{bmatrix} l_7 & l_8 & l_9 \\ l_4 & l_5 & l_6 \\ l_1 & l_2 & l_3 \end{bmatrix}, \tag{5.21}$$

with constant coefficients, i.e., independent of $x \in \Omega_k$. Let P_k be defined by

$$P_k = \begin{bmatrix} \alpha & \frac{1}{2} + \mu & \delta \\ \frac{1}{2} - \lambda & 1 & \frac{1}{2} + \lambda \\ \gamma & \frac{1}{2} - \mu & \beta \end{bmatrix}, \tag{5.22}$$

with constant coefficients, i.e., independent of $x \in \Omega_{k-1}$; α, β, γ, δ are (again) defined by solving the homogeneous equation at the $\Omega_{k,(1,1)}$ points, λ and μ are still free to be chosen. Define $e_i \equiv l_i / l_5$, $i = 1, \ldots, 9$.

By means of (5.9) we obtain the equations:

$$\begin{aligned} \alpha &= -\left(e_3 + \tfrac{1}{2}e_2 + \tfrac{1}{2}e_5\right) + e_2\lambda - e_6\mu, & \beta &= -\left(e_7 + \tfrac{1}{2}e_4 + \tfrac{1}{2}e_8\right) - e_8\lambda + e_4\mu, \\ \gamma &= -\left(e_9 + \tfrac{1}{2}e_5 + \tfrac{1}{2}e_8\right) + e_8\lambda + e_6\mu, & \delta &= -\left(e_1 + \tfrac{1}{2}e_2 + \tfrac{1}{2}e_4\right) - e_2\lambda - e_4\mu. \end{aligned} \tag{5.23}$$

Lemma 5.15. (i) *Prolongation* (5.22), (5.23) *is identical to prolongation* (5.4) *if the system*

$$\begin{aligned} e_3 + \tfrac{1}{2}e_2 + \tfrac{1}{2}e_6 + \tfrac{1}{4} &= \left(e_2 + \tfrac{1}{2}\right)\lambda + \left(-e_6 - \tfrac{1}{2}\right)\mu, \\ e_7 + \tfrac{1}{2}e_4 + \tfrac{1}{2}e_8 + \tfrac{1}{4} &= \left(-e_8 - \tfrac{1}{2}\right)\lambda + \left(e_4 + \tfrac{1}{2}\right)\mu, \\ e_9 + \tfrac{1}{2}e_6 + \tfrac{1}{2}e_8 + \tfrac{1}{4} &= \left(e_8 + \tfrac{1}{2}\right)\lambda + \left(e_6 + \tfrac{1}{2}\right)\mu, \\ e_1 + \tfrac{1}{2}e_2 + \tfrac{1}{2}e_4 + \tfrac{1}{4} &= \left(-e_2 - \tfrac{1}{2}\right)\lambda + \left(-e_4 - \tfrac{1}{2}\right)\mu, \end{aligned} \tag{5.24}$$

is solvable for λ *and* μ;

(ii) *if* $\sum_{i=1}^{9} l_i = 0$, *then system* (5.24) *has rank* $\leqslant 3$;

(iii) *if* $\Sigma_{i=1}^{9} l_i = 0$ *and system* (5.24) *is solvable, then*

$$\tfrac{1}{2}+\lambda = \frac{l_1+l_4+l_7}{(l_1+l_4+l_7)+(l_3+l_6+l_9)}, \qquad \tfrac{1}{2}-\lambda = \frac{l_3+l_6+l_9}{(l_1+l_4+l_7)+(l_3+l_6+l_9)},$$

$$\tfrac{1}{2}+\mu = \frac{l_1+l_2+l_3}{(l_1+l_2+l_3)+(l_7+l_8+l_9)}, \qquad \tfrac{1}{2}-\mu = \frac{l_7+l_8+l_9}{(l_1+l_2+l_3)+(l_7+l_8+l_9)}.$$

Proof. Part (i) follows immediately from (5.4) and (5.23), part (ii) follows from adding the four equations, part (iii) is straightforward. □

Example 5.16. Let

$$L_k^* = \begin{bmatrix} \tau l_4 & \tau l_5 & \tau l_6 \\ l_4 & l_5 & l_6 \\ \tau l_4 & \tau l_5 & \tau l_6 \end{bmatrix} \quad \text{or} \quad L_k^* = \begin{bmatrix} \tau l_8 & l_8 & \tau l_8 \\ \tau l_5 & l_5 & \tau l_5 \\ \tau l_2 & l_2 & \tau l_2 \end{bmatrix},$$

with $\Sigma_{i=1}^{9} l_i = 0$ and $0 \leqslant \tau \leqslant 1$; then system (5.13) is solvable.

6. Implementation and computational cost

The present blackbox solver consists of a preparational stage and a cycling stage. An outline of the cycling stage using the sawtooth schedule can be found in [12, p.617], [10, p.148]. The preparational stage is formulated as follows (L_l is the matrix supplied by the user):

(1) **for** k **from** l **by** -1 **to** 2
(2) **do** compute and store weights a_k, b_k, c_k, d_k
(3) compute and store $L_{k-1} = R_{k-1} L_k P_k$
(4) **end do** (6.1)
(5) **for** k **from** 1 **to** l
(6) **do** compute and store ILLU-decomposition of L_k
(7) **end do**

If Ω_k is a rectangular $NX_k * NY_k$ grid, then the storage requirements for the weights are $2 * NX_k * NY_k$ reals and for the ILLU-decomposition $3 * NX_k * NY_k$ reals.

The efficient implementation of the Galerkin approximation L_{k-1} (line (3) of (6.1)) is a nontrivial task. An important equality is

$$R_{k-1} L_k P_k = R_{k-1}\left(I_k - I_k^{11}\right) L_k P_k, \tag{6.2}$$

which follows immediately from (5.7). By means of (6.2) the cost of computing L_{k-1} can be reduced with about 35 percent. If well implemented, the cost of computing L_{k-1} becomes asymptotically $29.25 * NX_k * NY_k$ multiplifications and 26.25 additions. On a vector computer:

$\frac{1}{2} NY_k$(117 VECTOR(*) + 105 VECTOR(+)) plus, for the CYBER 205,

$\frac{1}{2} NY_k$ 179 GATHER (length(VECTOR) = $\frac{1}{2} NX_k$, stride equals 2).

Table 6.1(a)
CPU-times (seconds) on the CYBER 750 (NOS/BE 1.5 LEVEL 587, FTN 5.1+564 compiler)

l	4	5
$NX_l = NY_l$	33	65
Weights a_k, b_k, c_k, d_k	0.040	0.158
Galerkin approximations	0.048	0.170
ILLU-decompositions	0.041	0.150
1 MG-cycle	0.048	0.155

Table 6.1(b)
CPU-times (seconds) on the CYBER 205 (one single vectorpipe, FORTRAN 200 CYCLE 654A compiler)

l	4	5	6
$NX_l = NY_l$	33	65	129
Weights	0.008	0.031	0.120
Galerkin approximations	0.015	0.037	0.102
ILLU-decompositions	0.011	0.031	0.107
1 MG-cycle	0.011	0.033	0.105

Table 6.1(c)
CPU-times (seconds) on the CRAY X-MP-24 (COS 1.16, CFT 1.15 compiler)

l	4	5	6
$NX_l = NY_l$	33	65	129
Weights	0.004	0.015	0.054
Galerkin approximations	0.002	0.007	0.016
ILLU-decompositions	0.004	0.012	0.037
1 MG-cycle	0.004	0.014	0.043

The code, called MGD9V, has been written in standard FORTRAN 77 and contains no machine-dependent features. Tables 6.1(a)–6.1(c) show CPU-times on different machines for the various tasks of MGD9V on all levels $1, \ldots, l$ together.

Note that the computation of coarse grid matrices (Galerkin Approximations) is extremely efficient on the CRAY. The reason is that the performance of the CRAY is not affected by strides > 1.

The question arises how MGD9V performs in comparison with a program based on the classical bilinear prolongation and restriction. Let MGSYM denote the program equivalent with MGD9V but based on (symmetric) bilinear prolongation and restriction. We find:

(i) 1 MG-cycle of MGD9V costs the same as 1 MG-cycle of MGSYM;

(ii) the preparational stage of MGD9V takes (less than) the work of 1 MG-cycle more than the preparational stage of MGSYM;

(iii) for easy problems MGD9V takes the same number of MG-cycles as MGSYM, for difficult problems MGD9V takes considerably less MG-cycles than MGSYM.

The first statement is obvious, the third statement follows from the experimental results in Section 7. With respect to (ii) we remark that the ILLU-decompositions will cost the same in both programs, the Galerkin approximations take fewer operations in MGD9V than in MGSYM but in MGSYM no weights have to be computed.

Another algorithm with similar objectives as MGD9V, in particular for diffusion problems, is an algorithm published by Kettler (cf. [7, §2.2]). We made our own implementation of his algorithm to which we refer here as MODMG. Results of experiments for several problems with MGSYM, MGD9V and MODMG are exhibited in Section 7. Compared with the cost of a MG-cycle of MODMG, the cost of a MG-cycle of MGD9V can be slightly less because of a cheaper evaluation of the prolongation at the $\Omega_{k,(1,1)}$ points.

The additional preparational work in MGD9V compared with MODMG, consists of the computation of the prolongation WEIGHTS which takes the amount of work of about one MG-cycle. However, the computation of the Galerkin approximations is probably more efficient in MGD9V.

7. Numerical results

In this section we demonstrate the robustness and efficiency of MGD9V and make a comparison with MGSYM (see Section 6) and MODMG, which is a program that follows the description of Kettler (cf. [7, §2.2]). Note that several of the test problems in this section are pure diffusion problems with Neumann boundary conditions, a full description of the discretization can be found in [1]. This type of problem results in a linear system with a singular matrix, the system is nevertheless solvable. This phenomenon is inherited by the coarse grid systems as was shown in Section 5. Therefore on the coarsest grid no direct solver can be used. Instead, 8 ILLU relaxation sweeps are applied. In the following, each testproblem is briefly described. The performance is measured by the number (n) of MG-cycles needed to reach a given reduction (red) of the l_2-norm of the residual, i.e., $\| r^{(n)} \|_2 < \text{red} * \| r^{(0)} \|_2$, where $r^{(k)}$ denotes the residual after k MG-cycles. All testproblems are taken from the literature, except Problem 4. For Problems 1–8 the initial guess is the zero solution, for Problems 9–11, on the inner area the initial guess is the zero solution and the initial solution on the boundary is given by the Dirichlet condition.

Problem 1. Poisson.
$-\Delta u = f$ on Ω,
$n \nabla u = 0$ on $\partial\Omega$ (Neumann),
$\Omega = (0, 32) \times (0, 32)$,
$f(8, 8) = f(24, 8) = f(8, 24) = f(24, 24) = -2$, $f(16, 16) = 8$, $f = 0$ otherwise.

l	Grid	red	MGSYM	MGD9V	MODMG
			n	n	n
4	33×33	10^{-9}	7	7	7

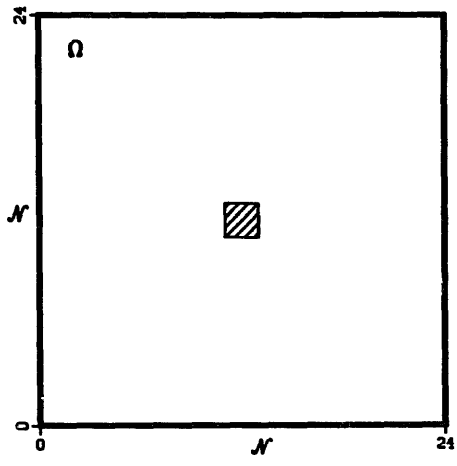

Fig. 7.1. Problem 3.

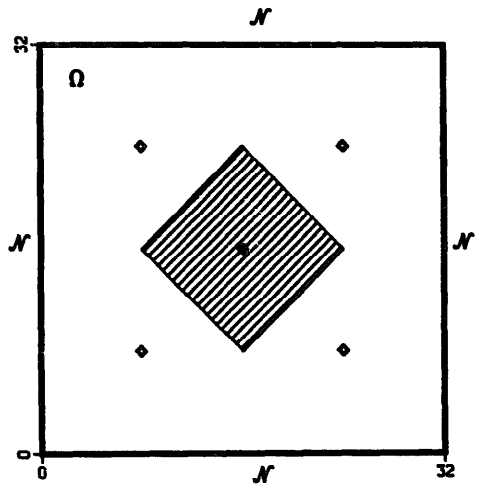

Fig. 7.2. Problem 4.

Problem 2. Hackbusch (cf. [4, p.217]).

$$-\Delta u + \frac{\partial^2}{\partial x_1 \partial x_2} u = 0 \quad \text{on } \Omega,$$

$\Omega = (0, 1) \times (0, 1)$.
Eliminated Dirichlet boundary conditions: $u = \sin(\pi x_1) + \sin(10\pi x_1) + \sin(\pi x_2) + \sin(10\pi x_2)$ on $\partial\Omega$, (special discretization cf. [4, p.217, §10.3.2]).

l	Grid	red	MGSYM	MGD9V	MODMG
			n	n	n
4	33×33	10^{-9}	6	8	19

Problem 3. The inhomogeneous square (see Fig. 7.1).

$$-\nabla D \nabla u = 1 \text{ on } \Omega,$$

$D = \frac{1}{3}$ outside the shaded region, $D = \frac{1}{3} \cdot 10^4$ inside the shaded region,

$$D\frac{\partial u}{\partial n} + \frac{1}{2}u = 0 \quad \text{on } \partial\Omega,$$

$\Omega = (0, 24) \times (0, 24)$ (cf. [1, p.450]).

l	Grid	red	MGSYM	MGD9V	MODMG
			n	n	n
4	25×25	10^{-9}	52	8	10

Problem 4. The inhomogeneous diamond (see Fig. 7.2).

$$-\nabla D \nabla u = 0 \text{ on } \Omega,$$

$D = 1$ outside the shaded region, $D = 10^5$ inside the shaded region.

$n\nabla u = 0$ on $\partial\Omega$ (Neumann),
$\Omega = (0, 32) \times (0, 32)$,
$f(8, 8) = f(24, 8) = f(8, 24) = f(24, 24) = -2$, $f(16, 16) = 8$, $f = 0$ otherwise.

The corners of the shaded region lie at (16, 8), (8, 16), (24, 16) and (16, 24). At $(ih, jh) \in \Omega - \partial\Omega$ the stencil of L_l is given by

$$\begin{bmatrix} & -d(\frac{1}{4}, \frac{1}{2}) - d(-\frac{1}{4}, \frac{1}{2}) & \\ -d(-\frac{1}{2}, \frac{1}{4}) - d(-\frac{1}{2}, -\frac{1}{4}) & -\text{SUM} & -d(\frac{1}{2}, \frac{1}{4}) - d(\frac{1}{2}, -\frac{1}{4}) \\ & -d(\frac{1}{4}, -\frac{1}{2}) - d(-\frac{1}{4}, -\frac{1}{2}) & \end{bmatrix},$$

where SUM is the sum of the off-diagonal elements and $d(p, q)$ is defined by $d(p, q) = \frac{1}{2}D((i+p)h, (j+q)h)$.

l	Grid	red	MGSYM	MGD9V	MODMG
			n	n	n
4	33×33	10^{-8}	18	7	7

Problem 5. The inhomogeneous staircase (see Fig. 7.3).

$$-\nabla D \nabla u = f \text{ on } \Omega = (0, 16) \times (0, 16).$$

$D = 1$ and $f = 0$ outside the shaded region, $D = 10^3$ and $f = 1$ inside the shaded region. $n\nabla u = 0$ on $x_1 = 0$ and on $x_2 = 0$ (Neumann), and

$$D\frac{\partial u}{\partial n} + \tfrac{1}{2}u = 0 \quad \text{on } x_1 = 16 \text{ and on } x_2 = 16$$

(cf. [1, p.453]).

l	Grid	red	MGSYM	MGD9V	MODMG
			n	n	n
3	17×17	10^{-9}	130	9	10

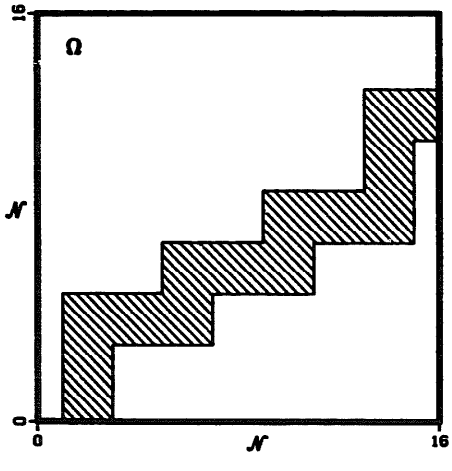

Fig. 7.3. Problem 5.

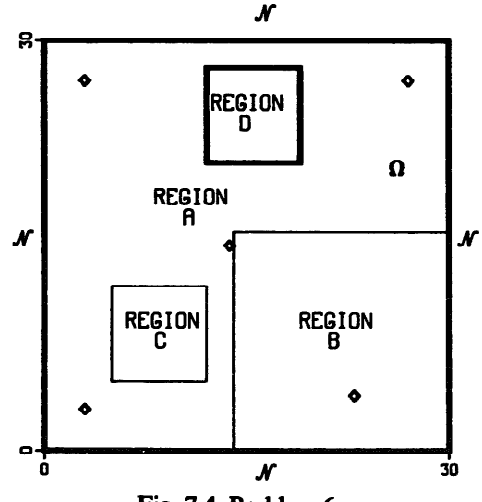

Fig. 7.4. Problem 6.

Problem 6. Stone's problem (cf. [11]) (see Fig. 7.4).

$$-\nabla D\nabla u = f \text{ on } \Omega = (0, 30) \times (0, 30),$$

$n\nabla u = 0$ on $\partial\Omega$ (Neumann),

$$D = \begin{pmatrix} d_{11} & 0 \\ 0 & d_{22} \end{pmatrix},$$

Region	A	B	C	D
d_{11}	1	1	10^5	0
d_{22}	1	10^5	1	0

$f(3, 3) = 1$, $f(23, 4) = 0.6$, $f(14, 15) = -1.83$, $f(3, 27) = 0.5$, $f(27, 27) = -0.27$, $f = 0$ otherwise.

For the region Ω a 31×31 grid is used. In order to be able to use 4 levels in the multigrid algorithms, virtual grid points are added to extend the grid to obtain a 33×33 grid (padding). In these points the difference stencil is given by

$$\begin{bmatrix} 0 & 0 & 0 \\ 0 & 1 & 0 \\ 0 & 0 & 0 \end{bmatrix}$$

and the right-hand side is zero. Of course, these equations do not influence the solution of the original discrete problem. Note that for MGD9V these points correspond to zero weights, so that also on the coarser grids these points do not couple with points in Ω.

l	Grid	red	MGSYM	MGD9V	MODMG
			n	n	n
4	33×33	10^{-8}	39	8	8

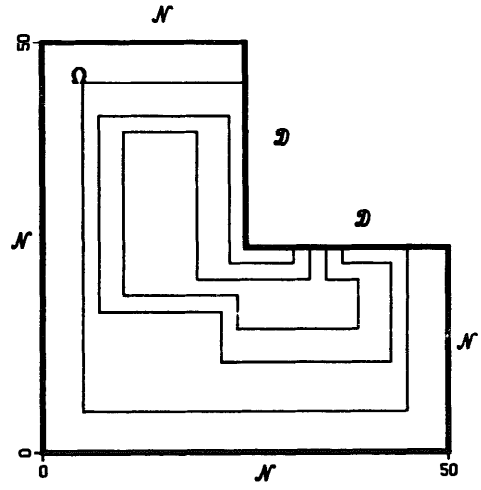

Fig. 7.5. Problem 7.

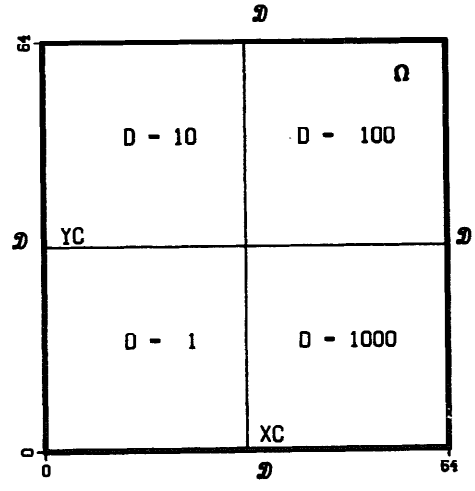

Fig. 7.6. Problem 8.

Problem 7. Kershaw's problem (cf. [6]) (see Fig. 7.5).

$$-\nabla D\nabla u + u = f \text{ on } \Omega,$$

$\Omega = ((0, 50) \times (0, 25)) \cup ((0, 25) \times (25, 50))$,
$u = 0$ (Dirichlet) on $\{(x_1, 25) \mid 25 \leqslant x_1 \leqslant 50\}$ and on $\{(25, x_2) \mid 25 \leqslant x_2 \leqslant 50\}$, $n \nabla u = 0$ elsewhere on $\partial\Omega$.

D increases discontinuously from the outer shell to the inner shell with the values 10^{-4}, 10^{-2}, 10, 10^6, $f(x_1, x_2) = 10^{(x_1 - x_2)/24.5 + 2}$.

With the same procedure as in Problem 6 the grid is extended by padding to a 65–65 grid.

l	Grid	red	MGSYM	MGD9V	MODMG
			n	n	n
5	65×65	10^{-9}	26	10	24

Problem 8. The four-corner junction (see Fig. 7.6).

$$-\nabla D\nabla u = f \text{ on } \Omega = (0, 64) \times (0, 64),$$

$$D\frac{\partial u}{\partial n} + \tfrac{1}{2}u = 0 \text{ on } \partial\Omega,$$

$$\left.\begin{matrix} 0 \leqslant y \leqslant yc \\ 0 \leqslant x \leqslant xc \end{matrix}\right\} D = 1,\ f = 0, \qquad \left.\begin{matrix} 0 \leqslant y \leqslant yc \\ xc < x \leqslant 64 \end{matrix}\right\} D = 10^3,\ f = -1,$$

$$\left.\begin{matrix} yc < y \leqslant 64 \\ 0 \leqslant x \leqslant xc \end{matrix}\right\} D = 10,\ f = 1, \qquad \left.\begin{matrix} yc < y \leqslant 64 \\ xc < x \leqslant 64 \end{matrix}\right\} D = 10^2,\ f = 0,$$

(cf. [9, p.197]).

l	Grid	red	MGSYM	MGD9V	MODMG
			n	n	n
5	65×65 $(xc,yc) = (32,32) \in \Omega_{5,(0,0)}$	10^{-8}	14	14	6
5	65×65 $(xc,yc) = (33,32) \in \Omega_{5,(1,0)}$	10^{-8}	14	7	6
5	65×65 $(xc,yc) = (32,31) \in \Omega_{5,(0,1)}$	10^{-8}	15	12	7
5	65×65 $(xc,yc) = (33,31) \in \Omega_{5,(1,1)}$	10^{-8}	15	7	DIV

DIV denotes divergence.

Problem 9. Convection diffusion (see Fig. 7.7).

$$-\epsilon\,\Delta u + a(x_1, x_2)\frac{\partial u}{\partial x_1} + b(x_1, x_2)\frac{\partial u}{\partial x_2} = 0 \quad \text{on } \Omega = (0, 1) \times (0, 1),$$

$u(x_1, x_2) = \sin(\pi x_1) + \sin(\pi x_2) + \sin(13\pi x_1) + \sin(13\pi x_2)$ on $\partial\Omega$ (Dirichlet boundary conditions), $a(x_1, x_2) = (2x_2 - 1)(1 - x_1^2)$, $b(x_1, x_2) = 2x_1x_2(x_2 - 1)$, $\epsilon = 10^{-5}$.

The characteristic directions which correspond to $a(\cdot)$ and $b(\cdot)$ are shown in Fig. 7.7.

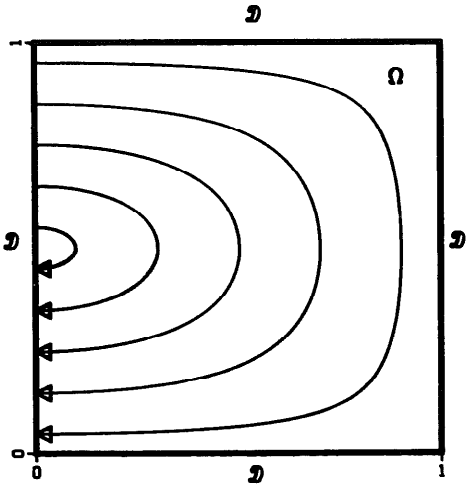

Fig. 7.7. Problem 9.

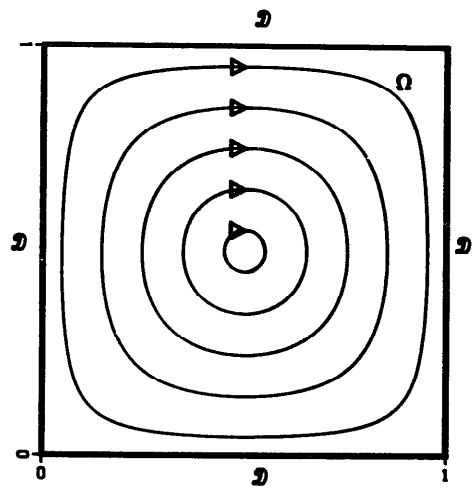

Fig. 7.8. Problem 10.

The problem and its discretization are the same as used by Ruge and Stüben [9, p.203].

l	Grid	red	MGSYM	MGD9V	MODMG
			n	n	n
4	33 × 33	10^{-8}	3	3	3
5	65 × 65	10^{-8}	DIV	3	4
6	129 × 129	10^{-8}		4	DIV

Problem 10. Convection diffusion (see Fig. 7.8).

$$-\epsilon\,\Delta u + a(x_1, x_2)\frac{\partial u}{\partial x_1} + b(x_1, x_2)\frac{\partial u}{\partial x_2} = 0 \quad \text{on } \Omega = (0, 1) \times (0, 1),$$

$u(x_1, x_2) = \sin(\pi x_1) + \sin(13\pi x_1) + \sin(\pi x_2) + \sin(13\pi x_2)$ on $\partial\Omega$ (Dirichlet boundary conditions),

$$a(x_1, x_2) = 4x_1(x_1 - 1)(1 - 2x_2),\ b(x_1, x_2) = -4x_2(x_2 - 1)(1 - 2x_1),\ \epsilon = 10^{-5}.$$

The characteristic directions which correspond to $a(\cdot)$ and $b(\cdot)$ are shown in Fig. 7.8. The problem and its discretization are the same as used by Ruge and Stüben [9, p.203]. Notice the stagnation point and notice that merely by numerical diffusion the solution of the discrete problem is unique.

l	Grid	red	MGSYM	MGD9V	MODMG
			n	n	n
4	33 × 33	10^{-8}	7	15	25
5	65 × 65	10^{-8}	11	17	39
6	129 × 129	10^{-8}	24	22	DIV

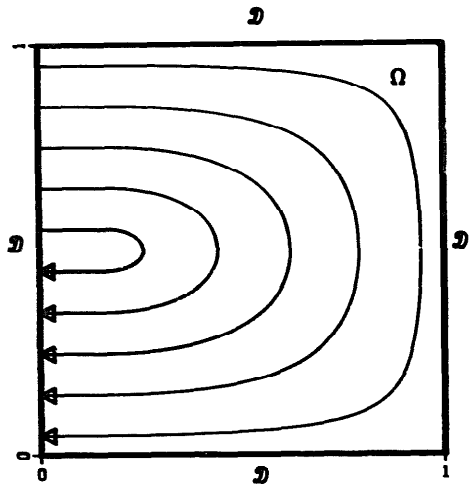

Fig. 7.9. Problem 11.

Problem 11. Convection diffusion (see Fig. 7.9).

$$-\epsilon\,\Delta u + a(x_1, x_2)\frac{\partial u}{\partial x_1} + b(x_1, x_2)\frac{\partial u}{\partial x_2} = 0 \quad \text{on } \Omega = (0, 1)\times(0, 1),$$

$u(x_1, x_2) = \sin(\pi x_1) + \sin(13\pi x_1) + \sin(\pi x_2) + \sin(13\pi x_2)$ on $\partial\Omega$ (Dirichlet boundary conditions),

$$a(x_1, x_2) = \begin{cases} (2x_2 - 1)(1 - \bar{x}_1^2) & \text{if } \bar{x}_1 > 0, \\ (2x_2 - 1) & \text{if } \bar{x}_1 \leqslant 0, \end{cases} \qquad b(x_1, x_2) = \begin{cases} 2\bar{x}_1 x_2(x_2 - 1) & \text{if } \bar{x}_1 > 0, \\ 0 & \text{if } \bar{x}_1 \leqslant 0, \end{cases}$$

where $\bar{x}_1 = 1.2x_1 - 0.2$, $\epsilon = 10^{-5}$.

The characteristic directions which correspond to $a(\cdot)$ and $b(\cdot)$ are shown in Fig. 7.9. The problem and its discretization are the same as used by Ruge and Stüben [9, p.203]. Notice the presence of a stagnation point.

l	Grid	red	MGSYM	MGD9V	MODMG
			n	n	n
4	33 × 33	10^{-8}	3	3	3
5	65 × 65	10^{-8}	DIV	4	4
6	129 × 129	10^{-8}		5	DIV

8. Conclusions

In this paper the attention has been focussed on improving the usual geometric multigrid method for solving the linear systems that arise from 9-points discretizations of elliptic PDEs in two dimensions. Improvement is achieved by automatic adaptation of prolongation and restriction operators to the particular discrete problem to be solved. Certain properties of the fine grid system are shown to be inherited by its coarse grid Galerkin approximation. The resulting code

MGD9V is both more robust and (for hard problems) far more efficient than a standard multigrid code based on the usual prolongation and restriction obtained by linear interpolation. The cost of a MG-cycle remains the same, and only some additional work is required in the preparational phase. This additional work is compensated by far by the decreased number of iterations. Also, if compared with the algorithm of Kettler (cf. [7]), MGD9V turns out to be an improvement. The code (written in ANSI FORTRAN 77) performs well also on vectorcomputers and especially on the CRAY. It is difficult to make a comparison with algebraic multigrid methods. If we consider AMG01 (cf. [9]), then, on the one hand, MGD9V will solve many problems from a large class (including hard problems) within the set-up time of AMG01. On the other hand, AMG01 is able to cope with larger stencils and irregular grids.

Acknowledgements

The author wishes to thank Prof. Dr. P.W. Hemker and Prof. Dr. P. Wesseling for their useful comments and careful reading of the manuscript. The author is indebted to Mr. W. Lioen for performing the experiments on the CRAY X-MP-24 needed for Table 6.1(c), and to Mr. M. Delussu who typed the manuscript.

References

[1] R.E. Alcouffe, A. Brandt, J.E. Dendy Jr. and J.W. Painter, The multi-grid method for the diffusion equation with strongly discontinuous coefficients, *SIAM J. Sci. Statist. Comput.* **2** (4) (1981) 430–454.

[2] A. Brandt, Multilevel adaptive solutions to boundary-value problems, *Math. Comp.* **31** (1977) 333–390.

[3] J.E. Dendy Jr, Blackbox multigrid for nonsymmetric problems, *Appl. Math. Comput.* **13** (1983) 261–283.

[4] W. Hackbusch, *Multi-grid Methods and Applications*, Springer Ser. Comput. Math. **4** (Springer, Berlin, 1985).

[5] P.W. Hemker and P.M. de Zeeuw, Some implementations of multigrid linear system solvers, in: D.J. Paddon and H. Holstein, Eds., *Multigrid Methods for Integral and Differential Equations*, Inst. Math. Appl. Conf. Ser. New Ser. (Oxford Univ. Press, New York, 1985) 85–116.

[6] D.S. Kershaw, The incomplete Cholesky-conjugate gradient method for the iterative solution of systems of linear equations, *J. Comput. Phys.* **26** (1978) 43–65.

[7] R. Kettler, Analysis and comparison of relaxation schemes in robust multigrid and preconditioned conjugate gradient methods, in: W. Hackbusch and U. Trottenberg, Eds., Lecture Notes in Math. **960** (Springer, Berlin, 1981) 502–534.

[8] R. Kettler and J.A. Meijerink, A multigrid method and a combined multigrid-conjugate gradient method for elliptic problems with strongly discontinuous coefficients in general domains, Shell Publ. 604, KSEPL, Rijswijk, The Netherlands, 1981.

[9] J. Ruge and K. Stüben, Efficient solution of finite difference and finite element equations by algebraic multigrid, in: D.J. Paddon and H. Holstein, Eds., *Multigrid Methods for Integral and Differential Equations*, Inst. Math. Appl. Conf. Ser. New Ser. (Oxford Univ. Press, New York, 1985) 169–212.

[10] P. Sonneveld, P. Wesseling and P.M. de Zeeuw, Multigrid and conjugate gradient methods as convergence acceleration techniques, in: D.J. Paddon and H. Holstein, Eds., *Multigrid Methods for Integral and Differential Equations*, Inst. Math. Appl. Conf. Ser. New Ser. (Oxford Univ. Press, New York, 1985) 117–167.

[11] H.L. Stone, Iterative solution of implicit approximation of multidimensional partial differential equations, *SIAM J. Numer. Anal.* **5** (3) (1968) 530–558.

[12] P. Wesseling, A robust and efficient multigrid method, in: W. Hackbusch and U. Trottenberg, Eds., Lecture Notes in Math. **960** (Springer, Berlin, 1981) 614–630.

[13] D.M. Young, *Iterative Solution of Large Linear Systems* (Academic Press, New York, 1971).

[14] P.M. de Zeeuw and E.J. van Asselt, The convergence rate of multi-level algorithms applied to the convection-diffusion equation, *SIAM J. Sci. Statist. Comput.* **6** (2) (1985) 492–503.